Title

Correction to “Active Site Fluxional Restructuring as a New Paradigm in Triggering Reaction Activity for Nanocluster Catalysis”

Journal

Accounts of Chemical Research, 54(24)

ISSN

0001-4842

Authors

Sun, Geng
Sautet, Philippe

Publication Date

2021-12-21

DOI

10.1021/acs.accounts.1c00699

Peer reviewed

Active Site Fluxional Restructuring as a New Paradigm in Triggering Reaction Activity for Nanocluster Catalysis

Geng Sun[1], Philippe Sautet[1,2,*]

Email: sautet@ucla.edu

1. Department of Chemical and Biomolecular Engineering, University of California, Los Angeles, Los Angeles, California 90095, United States

2. Department of Chemistry and Biochemistry, University of California, Los Angeles, Los Angeles, California 90095, United States

1 Conspectus

The rationale of the catalytic activity observed in experiments is a crucial task in fundamental catalysis studies. Efficient catalyst design relies on the accurate understanding of the origin of the activity at the atomic level. Theoretical studies have been widely developed to reach such a fundamental atomic scale understanding of catalytic activity. Current theories ascribe the catalytic activity to the geometric and electronic structure of the active site, in which the geometrical and electronic structure effects are derived from the equilibrium geometry of active sites characterizing the static property of the catalyst, however catalysts, especially in the form of nanoclusters, may present fluxional and dynamic structure under reaction conditions and the effect of this fluxional behavior is not yet widely recognized. Therefore, this account will focus on the fluxionality of the active sites which is driven by thermal fluctuations under finite temperature. Under reaction conditions, nanocluster catalysts can readily restructure, either being promoted to another metastable isomer (named as plastic fluxionality) or presenting ample deformations around their equilibrium geometry (named as elastic fluxionality). This account summarizes our recent studies on the fluxionality of the nanoclusters and how plastic and elastic fluxionality play roles in highly efficient reaction pathways. Our results show that the low energy metastable isomers formed by plastic fluxionality can manifest a high reactivity despite their minor occurrence probability in the mixture of catalyst isomers. In the end, the highly active metastable isomer may dominate the total observed reactivity. In addition, the

isomerization between the global minimum structure and the highly active metastable isomer can be a central step in catalytic transformations in order to circumvents some difficult reaction steps and may govern the overall mechanism. In addition, the thermal fluctuation driven elastic fluxionality is also found to play a key role, in complement with plastic fluxionality. The elastic fluxionality creates substantial structural deformations of the active site, and these deformed geometries enable low activation energies and high catalytic activity, which cannot be found from the static, equilibrium geometry of the catalyst. A dedicated global activity search algorithm is proposed to search for the optimal reaction pathway on fluxional nanoclusters. In summary, our studies demonstrate that the thermal-driven fluxionality provides a different paradigm for understanding the high activity of nanoclusters under reaction conditions beyond the static description of geometric and electronic structure. We first summarize our previous results and then provide a perspective for further studies on how to investigate and take the advantage of the fluxional geometry of nanoclusters. We will defend in this account that the static picture for the active site is not complete, and might miss critical reaction pathways that are highly efficient and only open after thermally induced restructuring of the active site.

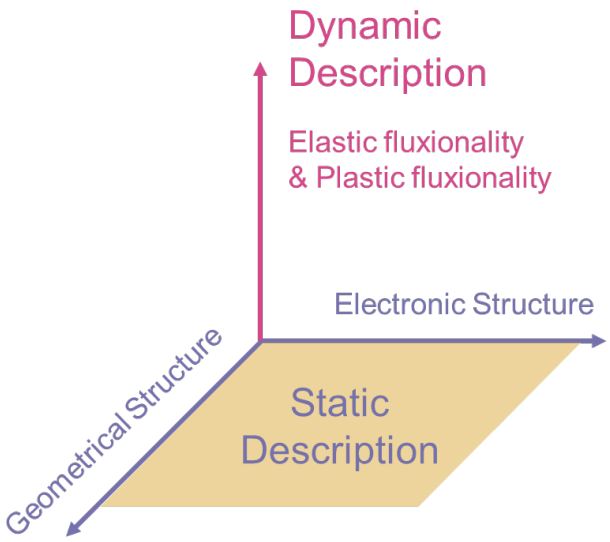

2 Key references

- Sun, G.; Sautet, P. Metastable Structures in Cluster Catalysis from First-Principles: Structural Ensemble in Reaction Conditions and Metastability Triggered Reactivity, J. Am. Chem. Soc. 2018, 140, 8, 2812–2820[1] *This article shows that a metastable isomer of hydrogenated Pt_{13} cluster could dominate total reactivity though its occurrence probability is rare.*
- Sun, G.; Fuller, J. T.; Alexandrova, A. N.; Sautet, P. Global Activity Search Uncovers Reaction Induced Concomitant Catalyst Restructuring for Alkane Dissociation on Model Pt Catalysts, ACS Catal. **2021**, 11, 1877-1885[2] *For a fluxional supported Pt_7 or Pt_8 catalyst under reaction conditions, not only the plastic fluxionality but the elastic fluxionality of the catalyst is crucial to obtain highly efficient active sites. The latter results in substantial thermal deformation of the catalyst structure, and leading to efficient reaction-reconstruction coupling mechanism. A global activity search method is designed for searching the optimal configuration of the active site on fluxional catalyst structure.*
- Sun, G.; Alexandrova, A. N.; Sautet, P. Structural Rearrangements of Subnanometer Cu Oxide Clusters Govern Catalytic Oxidation, ACS Catal. **2020**, 10, 9, 5309–5317[3] *In selective oxidation catalyzed by supported copper oxide clusters, an intermediate state of the catalyst is stable and very difficult to be reduced, while a feasible isomerization step between such as stable catalyst state and a highly active metastable isomer exists, and enables a highly efficient reaction mechanisms.*

3 Introduction

A fundamental understanding of the relationship between the attributes of catalytic sites and reaction activities is crucial for rational catalyst design. Currently, the most prevalent theories explain the origin of the catalytic activity using solely the static properties of the active sites, i.e. the electronic and geometric attributes of the equilibrium geometry. For the electronic effect, the *d* band model is a prevalent model linking the adsorption energy and the electronic structure (*d* state energies) of the active sites for transition metals.[4-5]. With the insights from *d* band model and Sabatier principle, one can improve the electronic structure of the active sites by ligand effect or

strain effect for better reactivity. For instance, a second element is generally alloyed with platinum for more efficient electrode material in oxygen reduction reaction.[6-8]

In complement to the electronic structure, the spatial arrangement of atoms at catalyst active sites generally has significant impacts on the reaction barriers. There are a few different well-established theories, from different scenarios, discussing the promotion of catalytic performance through geometric effects, such as the ensemble effect in the context of alloy catalysts requiring a group of active elements on the surface.[9] Another example is the B_5 site depicting a specific arrangement of five atoms in which three of them build a hollow site at the step bottom and two of them form a bridge site in step top region. The Ru B_5 site is particularly active for N_2 (or CO) activation.[10] Other examples include the bifunctional sites at the interfaces between metals and metal oxides.[11]

Rationalizing the catalytic activity by electronic and geometric effects is successful, [10, 12-14] however, the observation of the electronic structure and geometric structure relies on the equilibrium static geometry of the active sites. In realistic conditions, the atoms that comprise the active sites are constantly vibrating and diffusing, driven by thermal fluctuations. In many circumstances, such as high reaction temperature, one can expect nontrivial restructuring and fluxionality. We will review our recent studies on dynamical restructuring of the active site and its impact on catalytic activity, using the alkane dehydrogenation catalyzed by nanoclusters as examples. We will show that the dynamic properties of active sites could represent another key parameter to understand the reactivity of active sites, beyond the static description using the electronic structure and geometric effect.

4 Two types of fluxionality driven by thermodynamic fluctuations

To concentrate our discussions in this account within a precise context, we consider the phenomena of ample deformations of the active site structures promoted by thermal fluctuations as structural fluxionality. Thermal fluctuations may promote two loosely defined fluxional phenomena that coexist and are interconvertible. The first one refers to the active site structures vibrating and deforming around the equilibrium geometry but within a free energy basin. In this account, we will refer to this type of fluxional behavior as *elastic fluxionality* considering the forces always pull the structures back to

the equilibrium geometry. The second one refers to the structure restructuring into another free energy basin through a small barrier. At reaction temperatures, the isomerization of the structures from different basins is fast.[15] The second type of fluxional behavior is referred to as *plastic fluxionality* since external energy (thermal energy) is required to pull the structure back to the global minimum (GM) (Figure 1). By changing the reaction temperature, free energy basins may merge or become degenerate, and the plastic and elastic fluxionality will convert one to the other. The two types of fluxionality require different modelling methods. For the plastic fluxionality, one may use the local minima of each potential energy basin to represent the configurations of the whole basin following the simplified potential energy surface (PES) approach which reduces the effective dimension and saves the computational cost.[16] However, the elastic fluxionality requires explicit sampling of the configurations, which is computationally expensive. We will introduce the global activity search (GAS) method for studying the effect of elastic fluxionality on catalytic activity later in this account.[2]

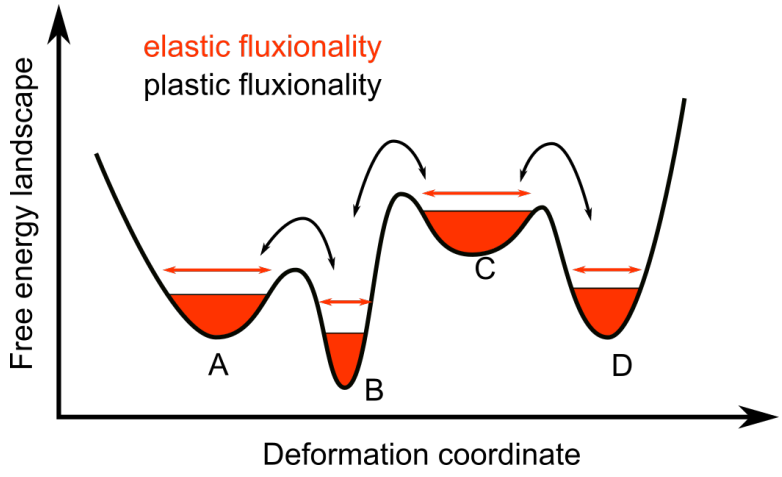

Figure 1 Two types of fluxional behaviors: elastic fluxionality and plastic fluxionality.

It is important to clarify the terminology *fluxionality* in this account with the terminology *dynamic* before continuing the discussion, because both are widely adopted in the literature for a wide range of distinguished physical phenomena. In this account, we will focus on the fluxional behavior of catalyst or active site driven by thermal fluctuations other than minimizing the free energy. In the literature, the restructuring of catalyst in varying temperatures or pressure, which changes the chemical potentials of gas-phase reactants, is also frequently referred to as the dynamic property of nanocluster catalysts. However, the adsorption induced reconstruction is

dominated by lowering the free energy of nanoclusters, which is different from the thermal fluctuation prompted fluxional dynamics focused in this account. The minimization of the free energy will result in a single GM structure, which has the largest occurrence probability. However, the fluxional motions of atoms are promoted by thermal fluctuations which activate the geometry from a single GM to higher (free) energy metastable isomers. On the other hand, the dynamics discussed in this account relies on the potential energy evaluated by Born–Oppenheimer and adiabatic state approximations, and we will not consider the non-adiabatic effect although it can also be a critical topic for catalytic reactions.[17]

5 Plastic fluxionality triggered reactivity

5.1 Metastability triggers the reactivity of hydrogenated Pt_{13} cluster toward methane activation.

To study the role of plastic fluxionality, which is characterized by the emergence of low-energy metastable isomers, global optimization methods are the key tools for identifying the probable local minimum structures as the first step. For example, we designed a modified genetic algorithm[1] for exploring the low-energy metastable ensemble (LEME, defined as the set of structures whose energies are within a given window from that of the GM) of hydrogenated Pt_{13} clusters. The energy spectrum of the LEME structures (using a 0.5 eV window) for Pt_{13}, $Pt_{13}H_{18}$, and $Pt_{13}H_{26}$ are shown in Figure 2. Pt_{13}, $Pt_{13}H_{18}$, and $Pt_{13}H_{26}$ have 49, 20, 19 unique structures in the LEME, respectively. Pt_{13} is the most fluxional system, showing different Pt cluster morphologies, while the LEME of $Pt_{13}H_{26}$ is characterized by a frozen cuboctahedral Pt_{13} core being blocked by various hydrogen decorations.

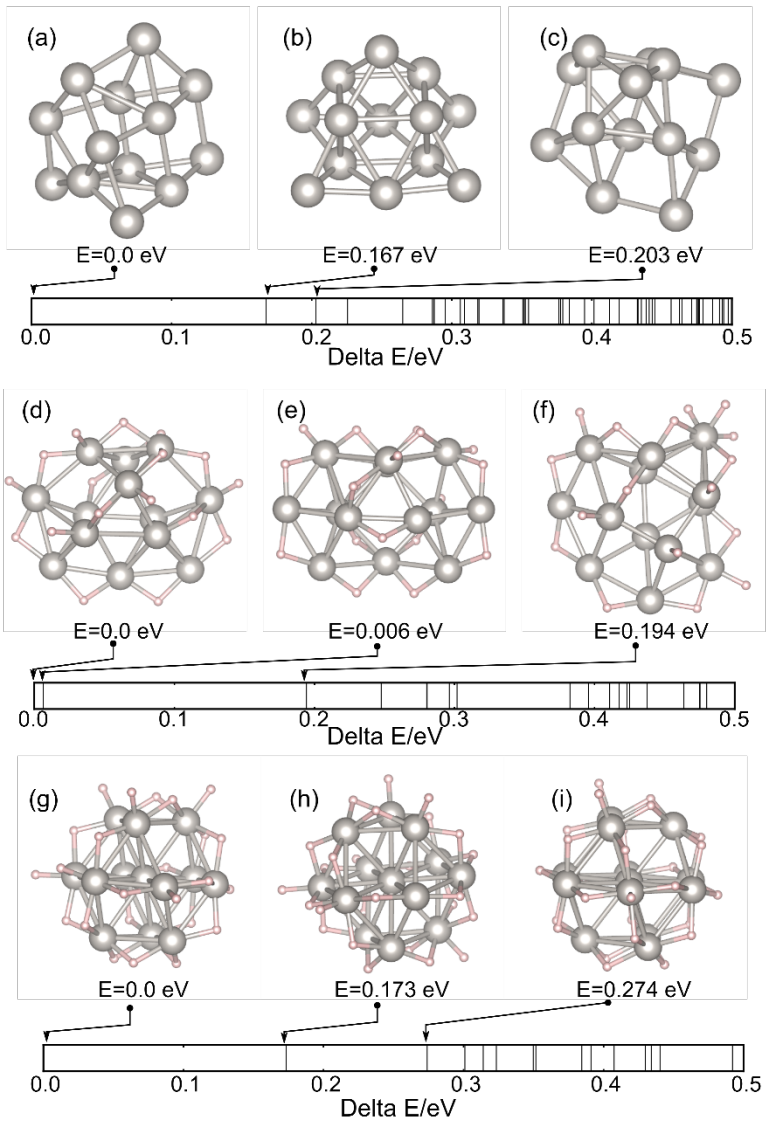

Figure 2 The low-energy metastable ensemble structures of three $Pt_{13}H_x$ clusters in 0.5 eV energy window. (a)-(c) show the first three most stable structures of Pt_{13}, (d)-(f) show the first three most stable structures of $Pt_{13}H_{18}$, (g)-(i) show the first-three most stable structures of $Pt_{13}H_{26}$. Under each row of structures, a spectrum of the energies of the low energy metastable ensemble are shown. The grey balls are Pt atoms and the light pink atoms are hydrogen atoms. Reproduced with permission from reference[1] Copyright 2018 American Chemical Society.

Starting from the knowledge of the presence of abundant metastable isomers, the next question to answer is the role of metastable isomers in catalysis. We first determined the optimal structure of $Pt_{13}H_x$ by *ab initio* thermodynamics, in which the reaction condition is selected as 400 °C and 0.5 bar of H_2, and found that $Pt_{13}H_{26}$ is the most stable configuration.[1] However, if we examine the details of the low energy metastable ensembles of $Pt_{13}H_{26}$, there are at least 19 unique isomers in the energy window from the energy of GM and 0.5 eV above (Figure 2). Hydrogen atoms adsorb on the top or bridge sites on the surface of the Pt_{13} cluster. The maximum Pt-H coordination number is 5 including 4 bridge H and 1 top H. We notice that the GM structure (GM0 in Figure

3) has two types of partially vacant Pt sites: PtH3 and PtH4 with a Pt-H coordination of 3 and 4, respectively. The PtH3 site misses a neighbor bridge H and a top H, and the PtH4 site misses the top H. The first metastable structure (GM1 in Figure 3(b)) also has the PtH3 and PtH4 site, while it possesses a special PtH2 site that has only two hydrogen neighbors. For the second metastable isomer (GM2 in Figure 3(b)), only PtH4 is present. The relative stabilities of the first three isomers of $Pt_{13}H_{26}$ are 0.0, 0.173, and 0.274 eV, respectively. Considering the reaction temperature, the relative occurrence probabilities of these isomers of the catalyst are 100 %, 5.1 %, 0.89 % using Boltzmann distribution. In typical experimental characterizations, the presence of GM1 and GM2 should be completely hidden behind the outstanding abundance of GM0. The experimentally observed activity would hence be routinely correlated with the GM0 isomer.

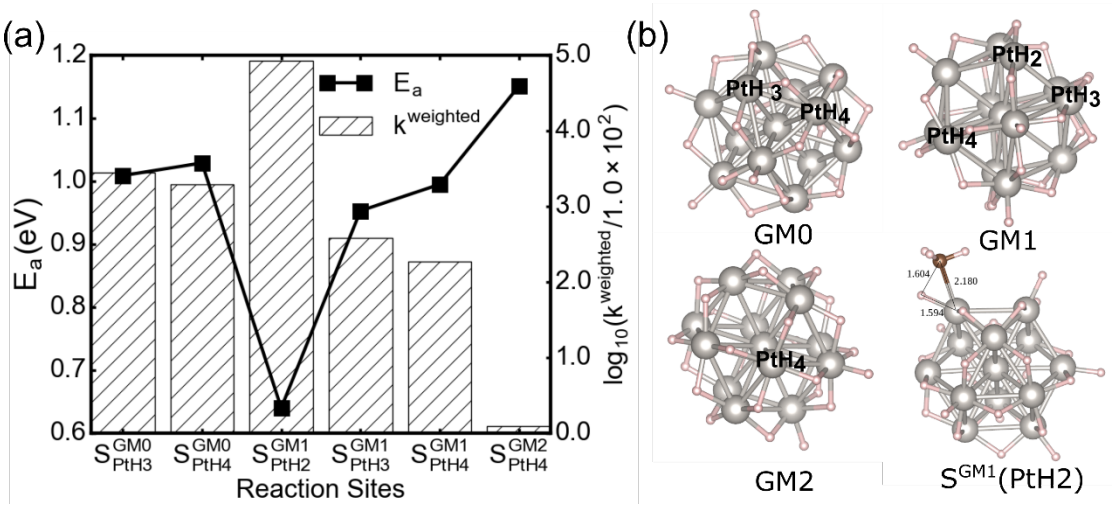

Figure 3 (a) Activation energy (E_a) and weighted reaction rates for methane C-H bond dissociation for the low energy metastable isomers of $Pt_{13}H_{26}$ clusters ($T = 400$ ℃); (b) structures of the first three low energy metastable isomers (the accessible active sites are shown) and transition state structure for methane C-H dissociation on the PtH2 site of the first metastable isomer (GM1). Adapted with permission from ref. 1. Copyright 2018 American Chemical Society.

To investigate the contributions of each isomer in catalytic reactions, the catalytic activity of the vacant Pt sites toward methane C-H activation is investigated. The two vacant Pt sites on GM0 are only moderately active for methane C-H dissociation showing barriers around 1.0 eV. However, on the first metastable isomer (GM1), the unique PtH2 site is proven to be very active for methane C-H dissociation and the barrier is around 0.6 eV, while the other PtH3 and PtH4 sites of GM1 show similar reaction barriers to that of GM0. The presence of the PtH2 site renders GM1 very active for methane activation, however, GM1 is only a minority structure with a small population because of its slightly less favorable energy. At high reaction temperature,

the relative population of GM0 and GM1 is supposed to be in equilibrium. Therefore, we exploit the occurrence probability of GM1 to weigh its intrinsic reaction rate,

$$r_w = pr_c = pAe^{-\frac{E_a}{k_B T}} \quad (1)$$

In Equation (1), p is the relative population of each isomer estimated by the Boltzmann distribution, A is the prefactor of the chemical reaction considered (we assume A is the same for all the surface sites), E_a is the barrier, T is the reaction temperature and k_B is the Boltzmann constant. Figure 3(a) shows r_w for methane activation on GM0, GM1 and GM2, and it is found that even though GM1 has a small population, the very high activity of the PtH2 site on GM1 still dominates the overall reaction rate. The weighted reaction rate through PtH2 site on the GM1 is 30 times faster than other reaction pathways. GM2 has only PtH4 site and is less active than GM0 for methane activation, hence GM2 is less probable and less active which is not interesting for the catalysis.

5.2 Structural isomers in the grand canonical ensemble

Under operando conditions, the adsorbate coverages on the active sites are varying from particle to particle, and from time to time, being dominated by thermal fluctuations. We still ascribe this structural diversity as plastic fluxionality since they are rooted in thermal fluctuations. To explore the structures of plastic fluxionality in the case of varying adsorbate coverages, grand canonical global optimization is necessary for exploring not only geometrical isomers but also compositional isomers. One example is the metal oxide clusters in O_2 environments, which may present different stoichiometries and reactivity. This is the case of the amorphous alumina supported Cu_4O_x clusters which present diverse stoichiometry and geometry (Figure 4), that have been acquired by the grand canonical Basin Hopping method.[3]

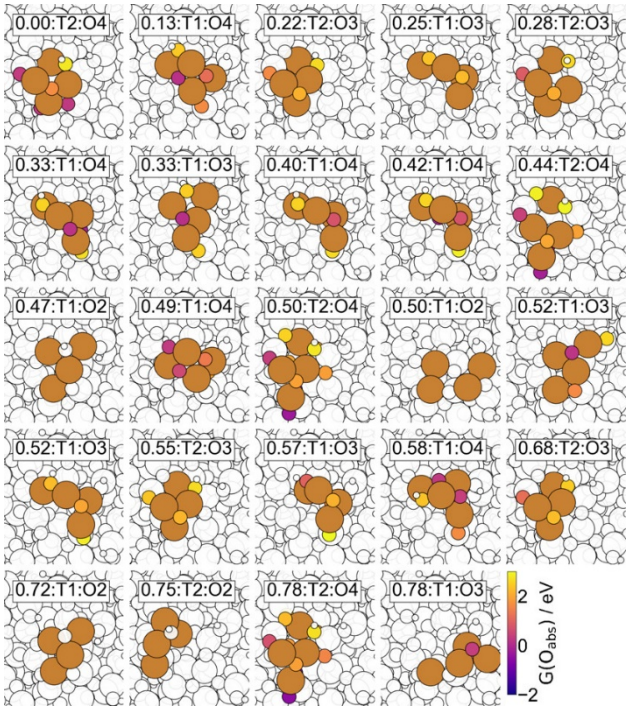

Figure 4 Top-view structures of the low free energy Cu_4O_x isomers. The relative free energies and number of oxygen atoms (x in Cu_4O_x) are also indicated. The brown balls are Cu atoms and the abstraction energy of oxygen atoms is color-coded. Oxygen atoms with large oxygen abstraction energy (> 3.0 eV) is are not colored (white). Other atoms are shown by white balls (large: Al, intermediate: support O, small: H). We distinguish two subgroups of clusters, type 1 (or T1) and type 2 (or T2), depending on their position on the support. Reproduced with permission from reference[3] Copyright 2020 American Chemical Society.

Such metal oxides can be used as catalysts for selective oxidation reactions, such as oxidative propane dehydrogenation (ODH)[18-19] and alkene epoxidation (EPO), in which reactant withdraws an oxygen atom from the active site and reduces the catalyst. e.g., the Cu_4O_x cluster is reduced to Cu_4O_{x-1} during reaction. To investigate the reactivity of all low free energy Cu_4O_x cluster isomers, the oxygen abstraction energy (ΔG^O_{abs}), which is the free energy difference between Cu_4O_x and Cu_4O_{x-1}, is computed. The Cu_4O_{x-1} cluster is obtained by removing one oxygen atom from the Cu_4O_x cluster and optimizing the Cu_4O_{x-1} structure into the immediate local minimum (rather than the global minimum of Cu_4O_{x-1}). ΔG^O_{abs} is defined in Equation (2), in which the chemical potential of the O_2 is computed by the ideal gas model.[3]

$$\Delta G^O_{abs} = G(\mathrm{Cu_4O_{x-1}}) - G(\mathrm{Cu_4O_x}) - \frac{1}{2}\mu(\mathrm{O_2}) \qquad (2)$$

The calculated ΔG^O_{abs} are shown in Figure 5 as a function of the clusters' formation energies. Cu_4O_x clusters present a large range of ΔG^O_{abs} from -1.20 to 5.10 eV. Oxygen

atoms with negative to moderate ΔG^{O}_{abs} (< 3.0 eV) are shown in both Figure 4 and Figure 5. Stoichiometry is the most crucial factor in determining the ΔG^{O}_{abs}. All Cu_4O_4 clusters, either type 1 or type 2, show at least one active oxygen with small ΔG^{O}_{abs} (< 0.5 eV). The small positive reaction free energy is readily compensated by the exothermic reaction energy from the selective oxidation reaction. Therefore, the catalyst reduction reaction $Cu_4O_4 \rightarrow Cu_4O_3$, combined with the selective oxidation reaction, propane dehydrogenation (ODH in Figure 5) or epoxidation (EPO in Figure 5) is exergonic, and is supposed to be a feasible step.

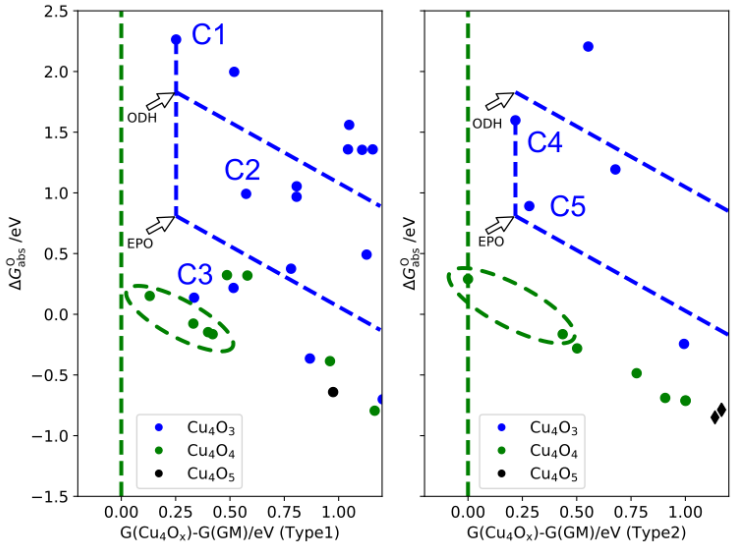

Figure 5 Each data point represents a supported Cu_4O_x cluster: the y coordinate is the smallest oxygen abstraction energy from the cluster and the x coordinate is the stability of the cluster indicated by the relative free energies using the GM as the reference (green dash lines). Colors of the point indicate the stoichiometry of the cluster, and the color codes are: Cu_4O_5 (black), Cu_4O_4 (green) and Cu_4O_3(blue). In the selected conditions (T=400 °C and p(O_2)=0.5 bar), the GM has the formula of Cu_4O_4. The left and right panel show the results from clusters of type 1 and type 2, respectively. Cluster isomers below (above) the blue dash lines would perform the oxidation reactions (propane ODH or propene EPO) exergonically (endergonically). Clusters in the green dash ellipse would be reduced to the most stable Cu_4O_3 in each type (C1 for type 1 and C4 for type 2). Adapted with permission from ref. 3. Copyright 2020 American Chemical Society.

The reduction of the first four most stable Cu_4O_4 clusters (green dots encompassed by a dashed ellipse in Figure 5(a)) produces a very stable Cu_4O_3 isomer (C1 blue dot in Figure 5). The minimal ΔG^{O}_{abs} of the cluster C1 is very large (~2.3 eV), and it is not possible to compensate such a large ΔG^{O}_{abs} by coupling with the ODH or EPO reactions. Therefore, the large ΔG^{O}_{abs} makes the reduction of Cu_4O_3 to Cu_4O_2 combined with the oxidation of the reactant a difficult endergonic step, which could be the rate-limiting step in the overall catalytic cycle. To circumvent this difficult reaction step, we examined the ΔG^{O}_{abs} of metastable Cu_4O_3 clusters. To investigate which metastable

isomers provide an alternative mechanism for bypassing the difficult step from C1, we decompose the reaction thermodynamics into three steps

$$Cu_4O_3(GM) \rightarrow Cu_4O_3(metastable) \qquad \Delta G_{iso} \qquad (3)$$

$$Cu_4O_3 \rightarrow Cu_4O_2 + \frac{1}{2}O_2 \qquad \Delta G^{O}_{abs} \qquad (4)$$

$$R + \frac{1}{2}O_2 \rightarrow RO \qquad \Delta G_R \qquad (5)$$

Equation (3) indicates the isomerization step leading to a metastable Cu_4O_3 isomer, equation (4) is linked with the oxygen abstraction energy, and equation (5) corresponds to the reaction energy of the targeted selective oxidation reaction. To find a metastable Cu_4O_3 structures that provides an alternative exergonic mechanism for the combined reactant oxidation and cluster reduction, the following equation must be met:

$$\Delta G_R + \Delta G^{O}_{abs} + \Delta G_{iso} < 0 \qquad (6)$$

Equation (6) sets up a boundary for the metastable isomers that can be potentially used. Figure 5 shows two boundary conditions which are associated to the reaction energy of ODH or EPO (blue dash lines). We find that there exists metastable Cu_4O_3 clusters only 0.1~ 0.3 eV higher than C1, but demonstrating a very active oxygen atom with ΔG^{O}_{abs} as +1 eV for C2 and +0.14 eV for C3, instead of +2.3 eV for C1. Hence C2 can be active species for ODH and C3 for ODH and EPO. Explicit reaction pathway searches for cluster restructuring event (Figure 6) shows that restructuring from C1 to C2 is kinetically fast (barrier 0.58 eV), confirming that this isomerization of Cu_4O_3 into a low energy metastable isomer is key to transform the poorly active GM of Cu_4O_3 into an active oxidation catalysts. The formation of Cu_4O_2 and its re-oxidation by O_2 reforms the initial Cu_4O_4 cluster catalyst, and hence closes the catalytic site.

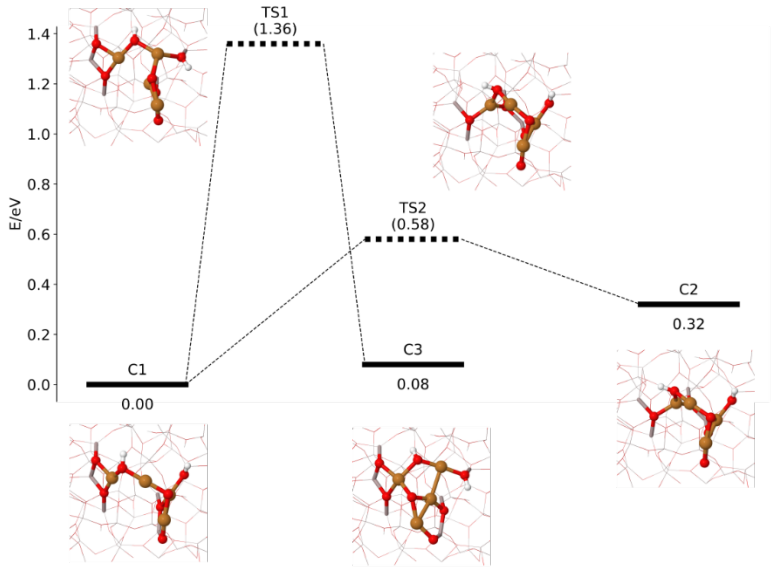

Figure 6 Isomerization pathways and barriers for Cu_4O_3 clusters. C1, C2 and C3 are three low free energy Cu_4O_3 clusters (see Figure 5). The brown balls are Cu atoms, the red balls are oxygen atoms, and the small white balls are hydrogen atoms. The details of alumina surface are hidden by thin line styles. Data from ref. 3.

6 The elastic fluxionality and concomitant reconstruction

We just showed that the plastic fluxionality of nanoclusters populates diverse metastable structures with different morphologies and compositions, and these metastable isomers, with specific geometrical and electronic properties, may dominate the catalytic activity, even though their population is low. Instead, the elastic fluxionality depicts the fluxional behavior of the cluster geometry within the same PES basin, around one local minimum, activated by thermal fluctuation. This section below will discuss the role of elastic fluxionality in catalysis using the example of alkane activation reaction catalyzed by small supported Pt clusters.

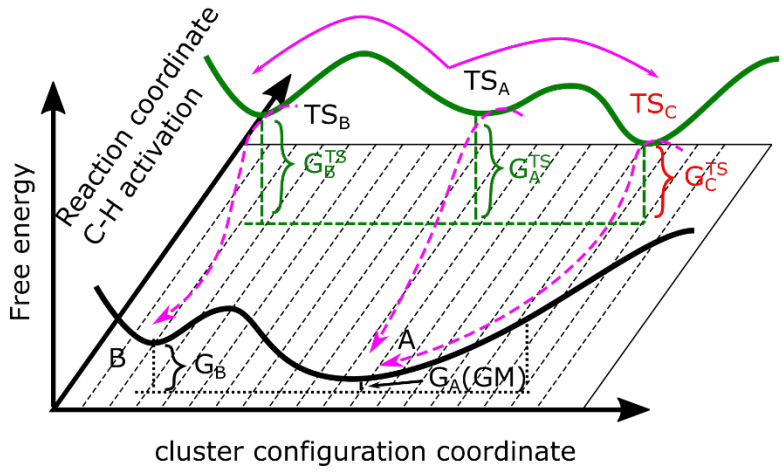

Figure 7 A schematic illustration of the GAS method. The GAS method directly explores and globally optimizes the configuration of the supported cluster and its adsorbates for the transition state (TS) of the considered catalytic elementary step, here C-H dissociation of methane (green line). From an existing TS (TS_A), GAS explores neighboring TS (TS_B or TS_C) by altering the adsorbate coverage or randomly displacing the coordinates of the supported cluster and adsorbates. The free energy difference between the new TS with new cluster configuration (TS_B or TS_C) and the original TS (TS_A) is used for determining whether the new TS is accepted or not. For each located TS structure, the "reactant state" configuration of the cluster, entry points of the reaction with methane far away of the cluster, are obtained by intrinsic reaction coordinate calculation. Adapted with permission from ref. 2. Copyright 2021 American Chemical Society.

Our recent study proposed a dedicated algorithm named the global activity search (GAS) method. Using alkane activation as an example, the GAS method globally optimizes the TS for the rate-determining step (C-H breaking of the alkane) and produces an ensemble of pathways including the transition states (TS) and entry clusters (ES) that initialized the pathway. The key characteristic of the GAS method is that it directly determines the configuration of the cluster catalyst that minimizes the energy of the TS for the considered catalytic reaction (green line in Figure 7) instead of stepwise exploring local minima on the PES and determining TS afterwards. In the example, the GAS method starts with an existing TS (TS_i) for alkane C-H activation catalyzed by supported Pt_8H_x nanocluster, then the GAS method manipulates hydrogen coverage of Pt_8 cluster as well as geometrical restructuring of the Pt_8 clusters. An algorithm is designed to optimize the distorted TS to another TS (TS_{i+1}) for methane activation. The free energies of the acquired TS ($G(TS_i)$ and $G(TS_{i+1})$) are used as the optimizing objective, and the standard Metropolis accepting rule can be implemented using the difference between the $G(TS_i)$ and $G(TS_{i+1})$. Finally, the GAS finds the putative lowest $G(TS_{opt})$ corresponding to the fastest reaction pathways in operando condition, where both the geometry and hydrogen coverage of the supported Pt_8H_x cluster catalyst are optimized. The entry clusters initializing the TSs can be computed afterward GAS by the intrinsic reaction coordinate method (magenta lines in Figure 7).

The GAS approach automatically generates a large number of reaction pathways for CH_4 activation catalyzed by Pt_8 cluster in the presence of the co-fed H_2 (the H adsorbate is in equilibrium with gas-phase H_2 at T=600 Celsius and P=0.1 bar). It should be noted that multiple reaction pathways may occur from the same Pt_8 isomer. Although the GM of Pt_8 has a formula of Pt_8H_6, we find that the optimal reaction pathway proceeds on a metastable configuration Pt_8H_5, highlighted by a green circle in Figure 8(a). What is more important, the optimal pathway for methane activation takes advantage of the elastic fluxionality of the cluster, as shown by the large distance variation color-coded in Figure 8(a). Figure 8(b) shows that in the optimal TS the elastic fluxionality enables Pt_8 to deform for optimizing the CH activation step. One Pt in the cluster is lifted away from the surface oxygen and gets electronically activated, and the top site hydrogen migrates to the neighbor bridge site to vacate the reaction site. Although the initial entry cluster shows a low reactivity, the thermal fluctuation promoted fluxionality, however, transforms the cluster into a different geometric and electronic structure that demonstrates the best reactivity for C-H dissociation. Since previous theoretical studies in the literature relied on electronic and geometrical structure of the equilibrium geometry, the new activity that originated from the fluctuation-driven fluxionality has been missed. Without the extensive sampling on the elastic fluxionality of the clusters, the reaction barrier for CH activation is overestimated by 0.26 eV.[2]

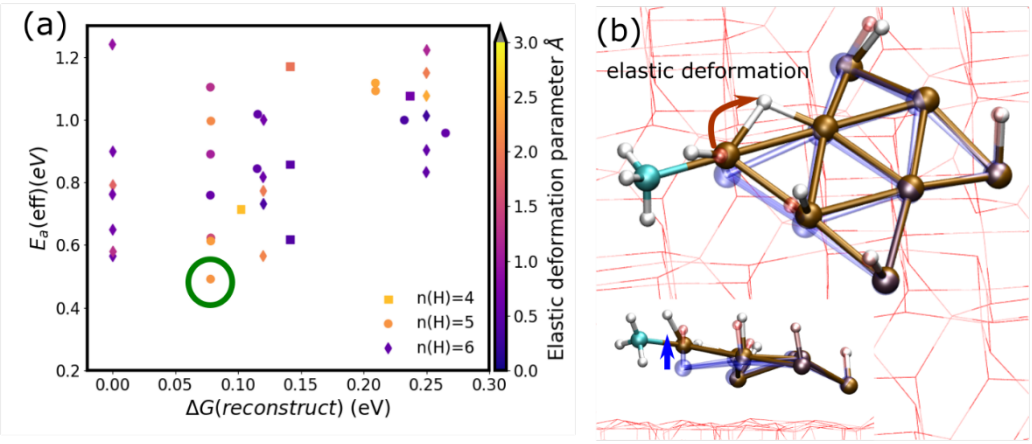

Figure 8 (a) illustrates the ensemble of pathways for methane activation catalyzed by alumina supported Pt_8H_n, generated by thermal fluxionality of the cluster catalyst. The x-axis shows the free energies of the entry clusters which initialize the reaction pathways. The y-axis shows the free energies of the TS for C-H dissociation. Symbol shape indicates the hydrogen coverage of the Pt_8 clusters. The color of the point codes the elastic deformation parameter (maximum displacement of a cluster atom during the reaction). (b) shows the elastic deformation of the cluster catalyst during the methane C-H bond dissociation for the lowest energy TS highlighted by a green circle in (a). Adapted with permission from ref. 2. Copyright 2021 American Chemical Society.

We should also note that the GAS has advantages over the metadynamics approach in computational efficiency, the capability of handling fluxionality in high-dimension configuration space, as well as the complexity from the grand canonical condition. More details are discussed in our previous publication.[2]

7 Summary and future opportunities

In this account, recent advances on the fluxional behavior of nanoclusters and its influence on catalytic performance have been presented and discussed. They show that besides the static property of the active sites, e.g. the electronic and geometric structure of the equilibrium geometry, the dynamic description of the active sites could play a key role in the catalytic activity, since thermal fluctuations can deform the catalytic site into a structure slightly less stable, but much more catalytically active. We can distinct two types of fluxionality activated by thermal fluctuation: plastic fluxionality and elastic fluxionality. The plastic fluxionality produces low-lying metastable isomers which could dominate the overall reactivity despite their low occurrence probability. Instead, elastic fluxionality results in a deformed geometry away from the equilibrium coordinates, and it is frequently ignored in the theoretical heterogeneous modeling. However, by using a dedicated global activity search method, our study shows that elastic fluxionality can play a key role on top of plastic fluxionality to provide low-lying transition states for catalytic elementary steps and highly active pathways in nanocluster catalysis, which cannot be found from a static description.

The concept of fluxionality assisted catalysis was demonstrated in this account on the basis of small supported subnanocluster catalysts, for which the active particle contains 4-13 atoms. Although these highly dispersed active phases can represent an important class of practical catalysts[20-23] and although fluxionality is very common, it is worthy to note that not all the catalysts can exhibit equivalently ample fluxionality.[24] In other situations when considering larger nanoparticles, although their core part is rather rigid, it can be expected that their surface atoms present substantial fluxionality at high temperature, as hinted by their surface premelting behavior.[25-26]

There are other outstanding questions. On one hand, in the example studies from this account, the fluxionality of the nanoclusters, either supported or isolated, are not controllable, and the potential energy landscape is the only factor influencing the mode

and magnitude of the fluxionality. Because of the high dimension of the potential energy surface and the large configuration space, not all fluxional behaviors will be beneficial to catalysis. Therefore, the next step could focus on finding ways to control and design the fluxional behavior for the active sites. Plausible strategies include reducing the size of the clusters to remove the unnecessary fluxional part, or limiting the nanoclusters in confined space where only a few beneficial fluxional modes are achievable. Atomistic simulations are valuable tools in exploring the atomistic details in this field.

On the other hand, it is important to strengthen the link with experimental observation. Considering the low population of metastable isomers and the short lifetime of the transient configuration from elastic deformation, it is very challenging to detect these minor species in the matrix of abundant global minima. Theoretical studies need to guide experiments for detecting the minor species that is the main player in the catalysis. For example, starting from the sampled atomic structures of the minorly populated metastable isomers, theoretical predictions can be used for predicting the spectroscopy of active species in X-ray absorption.[27] If the metastable active species presents unique electromagnetic response from the X-ray, they can be then distinguished from other spectators. Since the experimental spectrum always come from the mixture of active species and spectators, it is also important to demodulate the complex signals, and modulation excitation spectroscopy can be an important method in such a scenario. [28-30]

In addition, the fluxional behavior of the active sites being an intrinsic attribute of the potential energy of the atomic system and the reaction conditions, theoretical studies must rely on accurate and efficient potential energy evaluation methods as well as configuration sampling methods. The most popular methods, such as the brute-force *ab initio* molecular dynamic simulations are still too expensive to apply in catalysis studies. Well-established structural sampling algorithms such as Basin Hopping or genetic algorithms are not designed to cover all types of fluxional behaviors. Therefore, new developments that combine efficient potential energy evaluation methods, such as machine learning force field,[31] and fast configuration samplings methods[32] should be developed in the further studies.

8 Acknowledgments

This work was funded by the DOE-BES grant DE-SC0019152. This work used computational and storage services associated with the Hoffman2 Shared Cluster provided by the UCLA Institute for Digital Research and Education's Research Technology Group. This research used resources of the National Energy Research Scientific Computing Center (NERSC), a U.S. Department of Energy Office of Science User Facility operated under Contract No. DE-AC02-05CH11231. An award of computer time was provided by the Innovative and Novel Computational Impact on Theory and Experiment (INCITE) program. This research used resources of the Argonne Leadership Computing Facility, which is a DOE Office of Science User Facility supported under Contract DE-AC02-06CH11357.

9 Biographical Information

Dr. Geng Sun received his Bachelor degree in Peking University in 2011, and he also received his Ph.D. in Peking University in 2016. After that, he joined the group of Prof. Philippe Sautet as a post-doc researcher in University of California, Los Angeles for the study of catalysis on dynamic nanoclusters in ambient atmosphere.

Prof. Dr. Philippe Sautet has studied at "Ecole Polytechnique" in Paris and defended his doctorate in Theoretical Chemistry at Orsay University (Paris XI) in 1989. He then entered CNRS at the Institute of Research on Catalysis in Lyon, where he developed and lead a group devoted to the applications of theoretical chemistry to heterogeneous catalysis. After being the director of the laboratory of Chemistry at the ENS of Lyon for 8 years, he was director of the "Institut de Chimie de Lyon", a cluster of chemistry laboratories in Lyon, from 2007 to 2015. Philippe Sautet is now Distinguished Professor at the Chemical and Biomolecular Engineering department and at the Chemistry and Biochemistry department of the University of California, Los Angeles.

10 References

1. Sun, G.; Sautet, P., Metastable Structures in Cluster Catalysis from First-Principles: Structural Ensemble in Reaction Conditions and Metastability Triggered Reactivity. *Journal of the American Chemical Society* **2018**, *140*, 2812-2820.

2. Sun, G.; Fuller, J. T.; Alexandrova, A. N.; Sautet, P., Global Activity Search Uncovers Reaction Induced Concomitant Catalyst Restructuring for Alkane Dissociation on Model Pt Catalysts. *ACS Catalysis* **2021**, *11*, 1877-1885.

3. Sun, G.; Alexandrova, A. N.; Sautet, P., Structural Rearrangements of Subnanometer Cu Oxide Clusters Govern Catalytic Oxidation. *ACS Catalysis* **2020**, *10*, 5309-5317.

4. Bligaard, T.; Nørskov, J. K., Ligand Effects in Heterogeneous Catalysis and Electrochemistry. *Electrochimica Acta* **2007**, *52*, 5512-5516.

5. Hammer, B.; Norskov, J. K., Why Gold Is the Noblest of All the Metals. *Nature* **1995**, *376*, 238-240.

6. Kulkarni, A.; Siahrostami, S.; Patel, A.; Nørskov, J. K., Understanding Catalytic Activity Trends in the Oxygen Reduction Reaction. *Chemical Reviews* **2018**, *118*, 2302-2312.

7. Bing, Y.; Liu, H.; Zhang, L.; Ghosh, D.; Zhang, J., Nanostructured Pt-Alloy Electrocatalysts for Pem Fuel Cell Oxygen Reduction Reaction. *Chemical Society Reviews* **2010**, *39*, 2184-2202.

8. Li, Z.; Ma, X.; Xin, H., Feature Engineering of Machine-Learning Chemisorption Models for Catalyst Design. *Catalysis Today* **2017**, *280*, 232-238.

9. Sachtler, W. M. H.; Santen, R. A. V., Surface Composition and Selectivity of Alloy Catalysts. In *Advances in Catalysis*, Eley, D. D.; Pines, H.; Weisz, P. B., Eds. Academic Press: 1977; Vol. 26, pp 69-119.

10. Van Santen, R. A., Complementary Structure Sensitive and Insensitive Catalytic Relationships. *Accounts of Chemical Research* **2009**, *42*, 57-66.

11. Graciani, J.; Mudiyanselage, K.; Xu, F.; Baber, A. E.; Evans, J.; Senanayake, S. D.; Stacchiola, D. J.; Liu, P.; Hrbek, J.; Sanz, J. F.; Rodriguez, J. A., Highly Active Copper-Ceria and Copper-Ceria-Titania Catalysts for Methanol Synthesis from Co_2. *Science* **2014**, *345*, 546-550.

12. Honkala, K.; Hellman, A.; Remediakis, I. N.; Logadottir, A.; Carlsson, A.; Dahl, S.; Christensen, C. H.; Norskov, J. K., Ammonia Synthesis from First-Principles Calculations. *Science* **2005**, *307*, 555-8.

13. Norskov, J. K.; Rossmeisl, J.; Logadottir, A.; Lindqvist, L.; Kitchin, J. R.; Bligaard, T.; Jonsson, H., Origin of the Overpotential for Oxygen Reduction at a Fuel-Cell Cathode. *J Phys Chem B* **2004**, *108*, 17886-17892.

14. Liu, Z. P.; Hu, P., General Rules for Predicting Where a Catalytic Reaction Should Occur on Metal Surfaces: A Density Functional Theory Study of C-H and C-O Bond Breaking/Making on Flat, Stepped, and Kinked Metal Surfaces. *J Am Chem Soc* **2003**, *125*, 1958-67.

15. Zhai, H.; Alexandrova, A. N., Local Fluxionality of Surface-Deposited Cluster Catalysts: The Case of Pt7 on Al2o3. *The Journal of Physical Chemistry Letters* **2018**, *9*, 1696-1702.

16. Wales, D. J.; Doye, J. P. K., Global Optimization by Basin-Hopping and the Lowest Energy Structures of Lennard-Jones Clusters Containing up to 110 Atoms. *The Journal of Physical Chemistry A* **1997**, *101*, 5111-5116.

17. Wodtke, A. M.; Tully, J. C.; Auerbach, D. J., Electronically Non-Adiabatic Interactions of Molecules at Metal Surfaces: Can We Trust the Born-Oppenheimer Approximation for Surface Chemistry? *Int. Rev. Phys. Chem.* **2004**, *23*, 513-539.

18. Sattler, J.; Ruiz-Martinez, J.; Santillan-Jimenez, E.; Weckhuysen, B. M., Catalytic Dehydrogenation of Light Alkanes on Metals and Metal Oxides. *Chemical Reviews* **2014**, *114*, 10613-10653.

19. Blasco, T.; Nieto, J. M. L., Oxidative Dehydrogenation of Short Chain Alkanes on Supported Vanadium Oxide Catalysts. *Appl. Catal. A-Gen.* **1997**, *157*, 117-142.

20. Singh, J.; Nelson, R. C.; Vicente, B. C.; Scott, S. L.; van Bokhoven, J. A., Electronic Structure of Alumina-Supported Monometallic Pt and Bimetallic Ptsn Catalysts under Hydrogen and Carbon Monoxide Environment. *Physical Chemistry Chemical Physics* **2010**, *12*, 5668-5677.

21. Vaarkamp, M.; Miller, J. T.; Modica, F. S.; Koningsberger, D. C., On the Relation between Particle Morphology, Structure of the Metal-Support Interface, and Catalytic Properties of $Pt/\Gamma\text{-}Al_2O_3$. *Journal of Catalysis* **1996**, *163*, 294-305.

22. Vajda, S.; Pellin, M. J.; Greeley, J. P.; Marshall, C. L.; Curtiss, L. A.; Ballentine, G. A.; Elam, J. W.; Catillon-Mucherie, S.; Redfern, P. C.; Mehmood, F.; Zapol, P., Subnanometre Platinum Clusters as Highly Active and Selective Catalysts for the Oxidative Dehydrogenation of Propane. *Nat Mater* **2009**, *8*, 213-6.

23. Kang, J. H.; Menard, L. D.; Nuzzo, R. G.; Frenkel, A. I., Unusual Non-Bulk Properties in Nanoscale Materials: Thermal Metal−Metal Bond Contraction of Γ-Alumina-Supported Pt Catalysts. *Journal of the American Chemical Society* **2006**, *128*, 12068-12069.

24. Vargas, A.; Santarossa, G.; Iannuzzi, M.; Baiker, A., Fluxionality of Gold Nanoparticles Investigated by Born-Oppenheimer Molecular Dynamics. *Physical Review B* **2009**, *80*, 195421.

25. Alarifi, H. A.; Atiş, M.; Özdoğan, C.; Hu, A.; Yavuz, M.; Zhou, Y., Determination of Complete Melting and Surface Premelting Points of Silver Nanoparticles by Molecular Dynamics Simulation. *The Journal of Physical Chemistry C* **2013**, *117*, 12289-12298.

26. Wang, N.; Rokhlin, S. I.; Farson, D. F., Nonhomogeneous Surface Premelting of Au Nanoparticles. *Nanotechnology* **2008**, *19*, 415701.

27. Joly, Y.; Bunău, O.; Lorenzo, J. E.; Galéra, R. M.; Grenier, S.; Thompson, B., Self-Consistency, Spin-Orbit and Other Advances in the Fdmnes Code to Simulate Xanes and Rxd Experiments. *Journal of Physics: Conference Series* **2009**, *190*, 012007.

28. Muller, P.; Hermans, L., Applications of Modulation Excitation Spectroscopy in Heterogeneous Catalysis. *Ind Eng Chem Res* **2017**, *56*, 1123-1136.

29. Ferri, D.; Newton, M. A.; Nachtegaal, M., Modulation Excitation X-Ray Absorption Spectroscopy to Probe Surface Species on Heterogeneous Catalysts. *Topics in Catalysis* **2011**, *54*, 1070.

30. Srinivasan, P. D.; Patil, B. S.; Zhu, H.; Bravo-Suárez, J. J., Application of Modulation Excitation-Phase Sensitive Detection-Drifts for in Situ/Operando Characterization of Heterogeneous Catalysts. *Reaction Chemistry & Engineering* **2019**, *4*, 862-883.

31. Sun, G.; Sautet, P., Toward Fast and Reliable Potential Energy Surfaces for Metallic Pt Clusters by Hierarchical Delta Neural Networks. *Journal of Chemical Theory and Computation* **2019**, *15*, 5614-5627.

32. Bisbo, M. K.; Hammer, B., Efficient Global Structure Optimization with a Machine-Learned Surrogate Model. *Physical Review Letters* **2020**, *124*, 086102.